Science Signaling AAAS

www.sciencesignaling.org/cgi/content/full/4/180/ra43/DC1

Supplementary Materials for

Sequential Phosphorylation of Smoothened Transduces Graded Hedgehog Signaling

Ying Su, Jason K. Ospina, Junzheng Zhang, Andrew P. Michelson, Adam M. Schoen, Alan Jian Zhu*

*To whom correspondence should be addressed. E-mail: zhua@ccf.org

Published 5 July 2011, *Sci. Signal.* **4**, ra43 (2011)
DOI: 10.1126/scisignal.2001747

The PDF file includes:

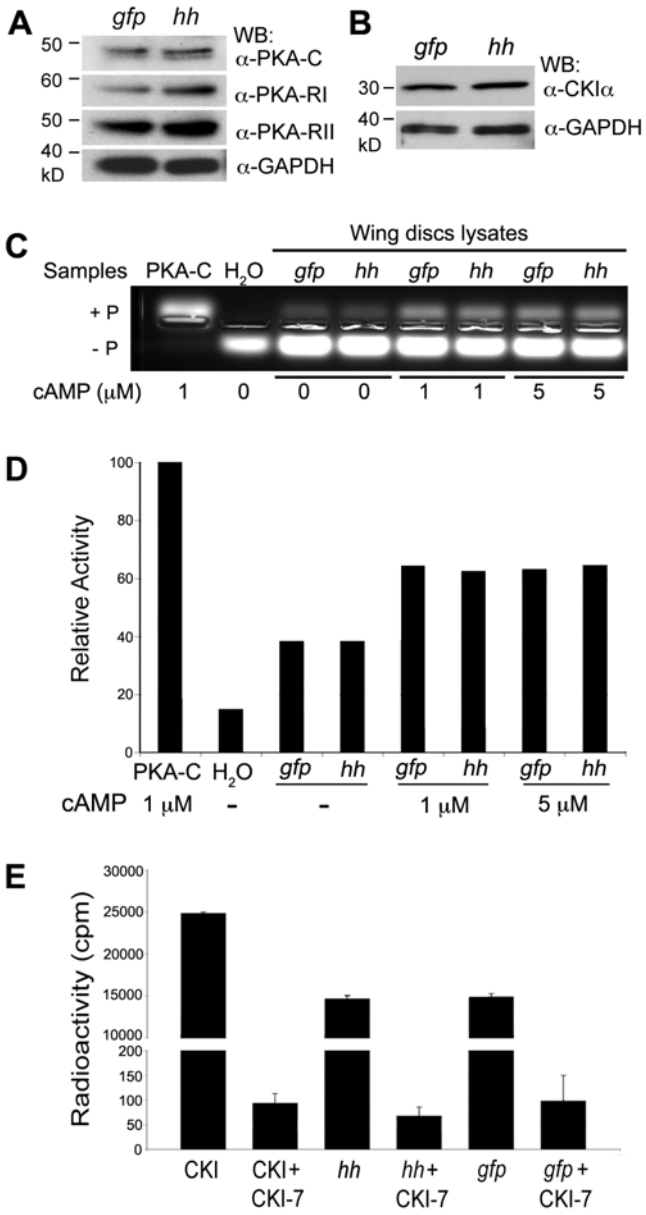

Fig. S1. Hh signaling does not affect PKA or CKI abundance or activity. (**A** and **B**) Western blotting (WB) analysis of the abundance of (A) PKA and (B) CKIα in wing discs overexpressing *gfp* or *hhN* driven by the *71B*-Gal4 driver at 29°C. No obvious differences in the abundances of the PKA catalytic subunit (PKA-C) or CKIα were observed; however, there was a slight increase in the abundance of the PKA regulatory (RI and RII) subunits in response to Hh (n = 3 experiments). GAPDH served as the loading control. (**C** and **D**) Increased Hh signaling has no effect on the activity of PKA. (**C**) Protein lysate (30 μg) from wing discs expressing *gfp* or *hhN* driven by *71B*-Gal4 at 29ºC were analyzed in the presence of different concentrations of cAMP. A representative agarose gel of the reaction products run with a PKA-specific fluorescence peptide substrate PepTag-LRRASLG (n = 3 experiments). Phosphorylation by PKA changes the net charge of the PepTag peptide, which enables the phosphorylated (+P) and non-phosphorylated (-P)

forms of the peptide to be rapidly separated on a 0.8% Tris-agarose gel. (**D**) PKA activities from the agarose gel shown in (C**)** were calculated relative to the activity of 0.2 units of the purified PKA catalytic subunit, which was the positive control. Water served as the negative control. (**E**) Increased Hh signaling has no effect on the activity of CKI. CKI activity was measured in triplicate from protein lysate (1 μg) from wing discs expressing *gfp* or *hhN* driven by *71B*-Gal4 at 29°C or 50 units of purified CKI (positive control) in the presence of the CKI substrate peptide (KRRRALpSVASLPGL) and [γ-^{32}P]-ATP. CKI-7 was used as a specific inhibitor of CKI. Relative CKI activity was determined by measuring the radioactivity of the phosphorylated substrate peptides (n = 3 experiments). Error bars represent standard deviations (SDs).

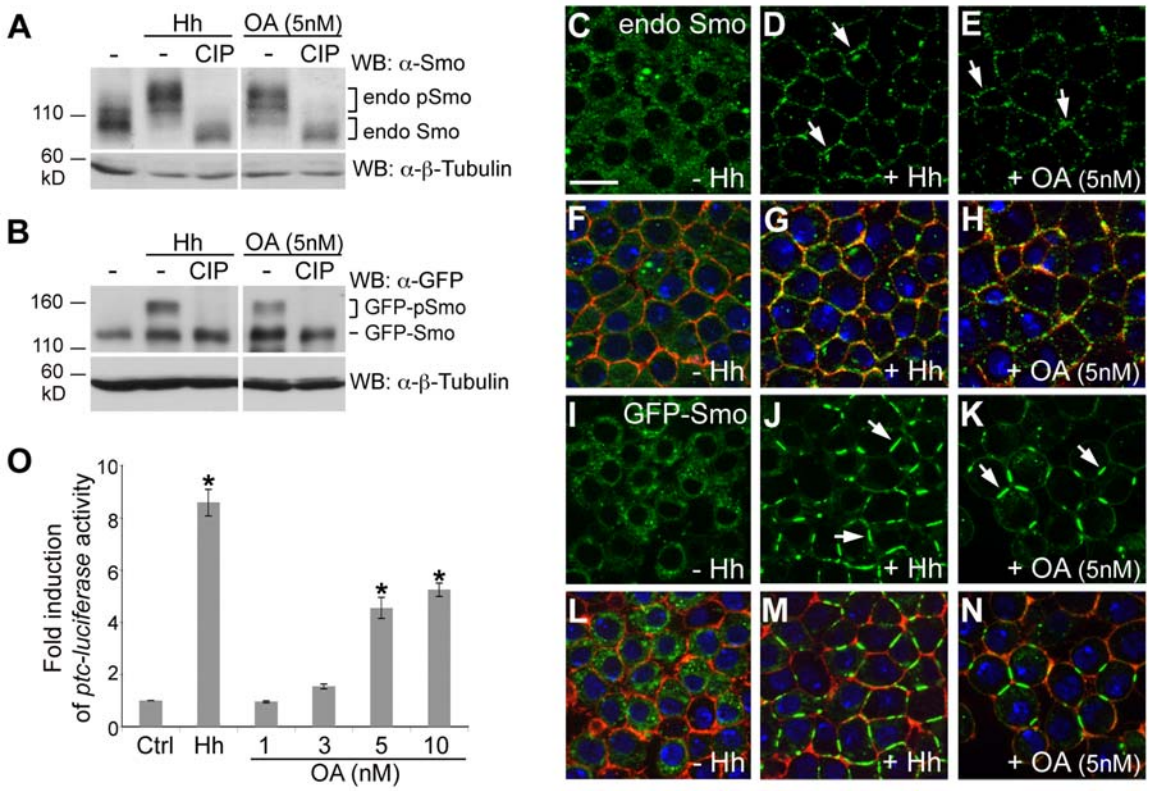

Fig. S2. Phosphatase activity regulates Smo signaling in cl-8 cells. (**A** and **B**) Phosphorylation of Smo in Hh- or OA-treated cl-8 cells. Slow migrating, phosphorylated forms of (A) endogenous Smo (endo pSmo) or (B) GFP-Smo (GFP-pSmo) were detected with a polyclonal antibody against Smo and an antibody against GFP in lysates from cl-8 cells or cl-8-gsmo cells treated with Hh-conditioned medium (Hh) or OA (5 nM) for 24 hours. A nonspecific phosphatase, calf intestinal phosphatase (CIP), was used as a positive control to remove pSmo. β-tubulin served as loading controls. (**C** to **N**) Surface localization of endogenous Smo (C to H) or GFP-Smo (I to N) in cl-8 or cl-8-*gsmo* cells treated with Hh for 24 hours or OA for 5 hours. Endogenous Smo (green) was detected with a monoclonal antibody against Smo (20C6) followed by biotin-streptavidin amplification (C to E). Note that both endogenous Smo (D and E) and GFP-Smo (J and K) displayed a particular enrichment at intercellular contacts (arrows), although this pattern was more striking for GFP-Smo, because we had to underexpose GFP-Smo micrographs to avoid saturation of GFP signals at intercellular contacts. Phalloidin (red) and DAPI (blue) marked the cell cortex and nuclei, respectively. Scale bar: 15 μm. (**O**) Luciferase assay for cl-8 cells transfected with the *ptc-luciferase* plasmid. After transfection, cells were treated with Hh or increasing amounts of OA for 24 hours, with the exception that cells treated with 10 nM OA were analyzed after 16 hours to minimize toxicity. Error bars represent SDs (n = 3 experiments). *, $P < 0.04$.

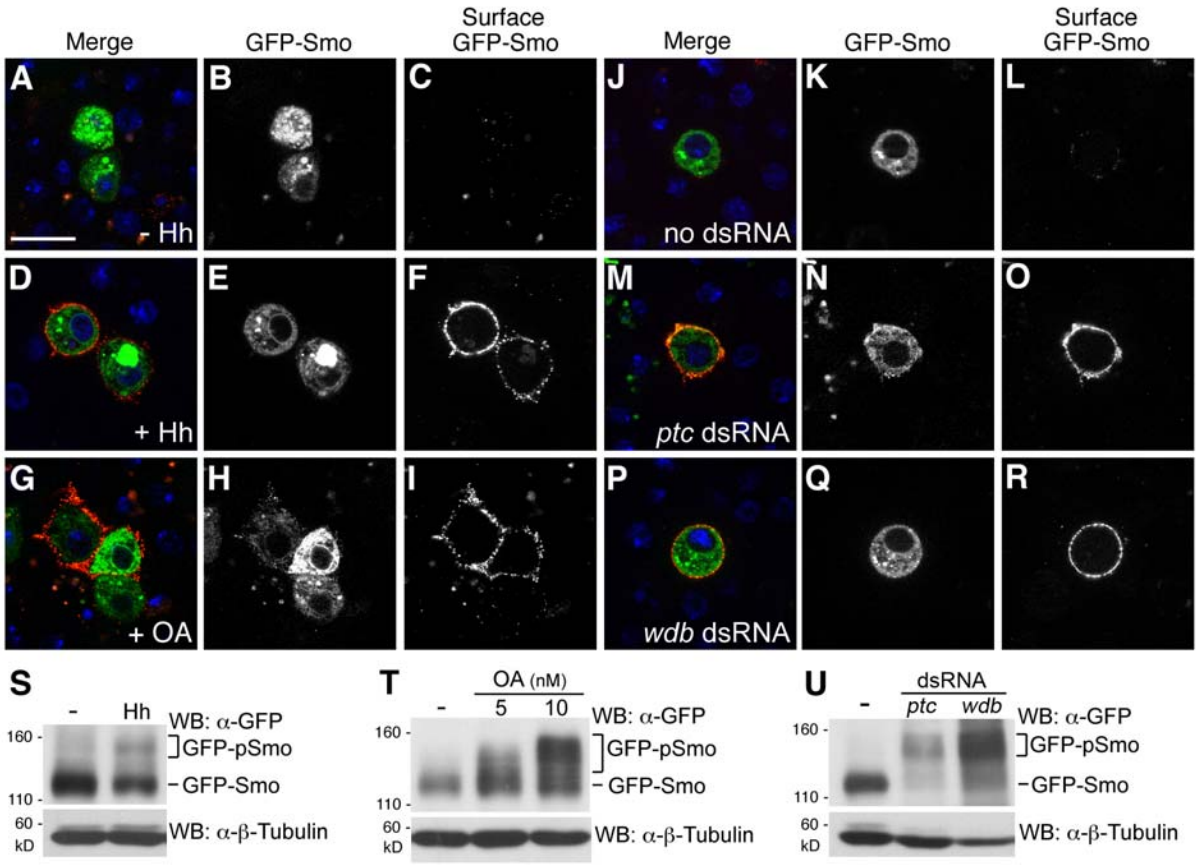

Fig. S3. Phosphatase activity regulates the phosphorylation and surface localization of Smo in S2 cells. *Drosophila* S2 cells, which lack *ci*, were transiently transfected with *gfp-smo*, followed by treatments with either Hh-conditioned medium (Hh), OA (10 to 50 nM), or the indicated dsRNAs. (**A** to **R**) Inhibiting PSTP function promotes the cell-surface localization of GFP-Smo in S2 cells. The localization of GFP-Smo was directly visualized by detecting GFP fluorescence. Surface-localized GFP-Smo (red) was detected by incubation with an antibody against Smo (20C6) without performing cell permeabilization. Ectopic GFP-Smo accumulated at the surface of S2 cells upon treatment with (D to F) Hh-conditioned medium or (M to O) *ptc* dsRNA. Inhibition of PP2A activity by (G to I) OA or (P to R) *wdb* dsRNA was sufficient to localize GFP-Smo to the surface of S2 cells. Note that 20C6 revealed a punctate staining pattern of surface localized GFP-Smo. Scale bar: 15 μm. (**S** to **U**) Inhibition of PSTP activity promotes Smo phosphorylation in S2 cells. Cell lysates were analyzed by Western blotting with an antibody against GFP to examine all forms of phosphorylated Smo (indicated by box brackets). Smo phosphorylation was induced in S2 cells treated with (S) Hh-conditioned medium, (T) OA, or (U) dsRNA targeting *ptc* or *wdb* (n = 4 experiments).

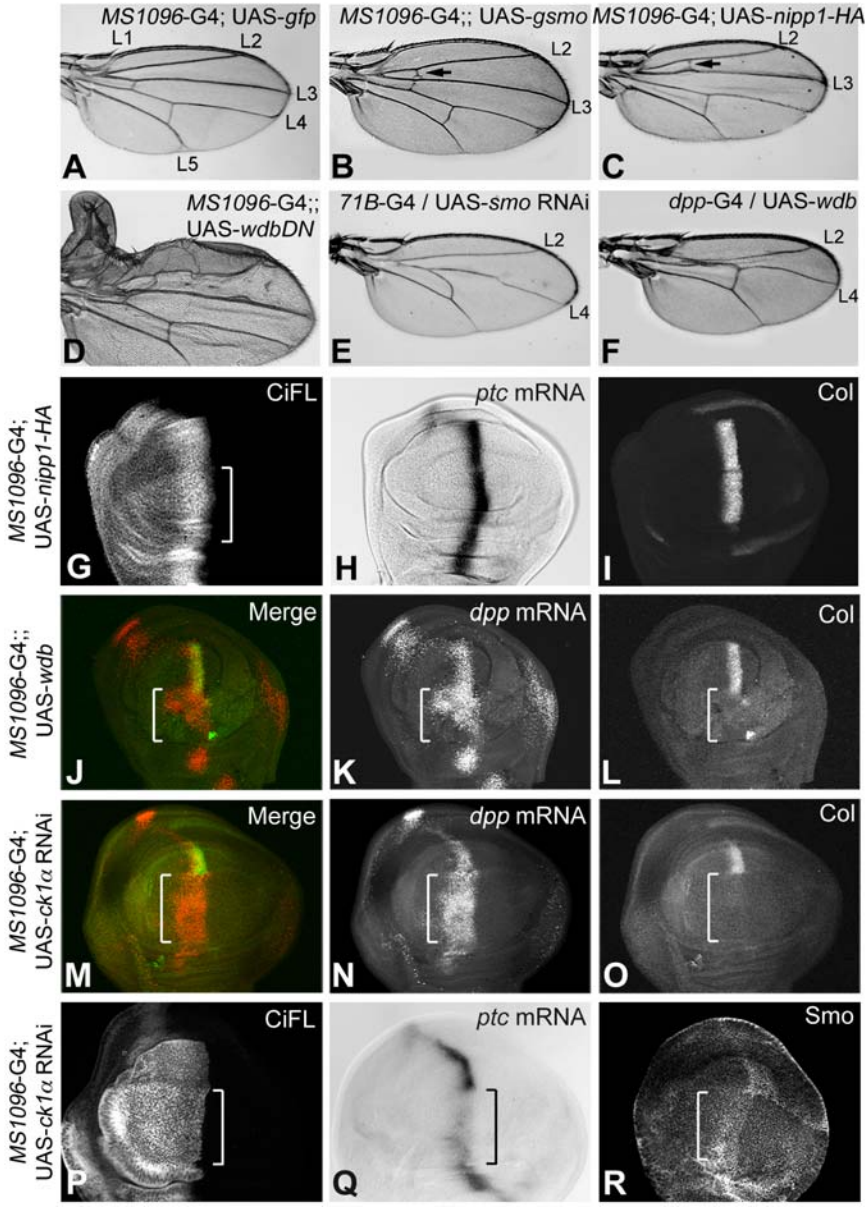

Fig. S4. Alteration of Hh signaling activity by manipulating the activities of Smo-specific kinases or phosphatases during *Drosophila* wing development. (**A** to **F**) Shown are wing blades of adult transgenic flies at 25°C. (B and C) Similar to *gsmo*, overexpression of the specific PP1 inhibitor *nipp1* induced the formation of an ectopic crossvein (arrows) between longitudinal veins L2 and L3. (D) Expression of *wdbDN* induced overgrowth of anterior wing structures, resembling a strong *hh* gain-of-function phenotype. (E) Inhibition of *smo* function by *smo* RNAi resulted in the loss of longitudinal vein L3. (F) This phenotype was phenocopied by overexpression of wild-type *wdb*. (**G** to **I**) Wing discs overexpressing *nipp1-HA* at 25°C, driven by *MS1096*-Gal4 (marked by box brackets), were subjected to in situ hybridization to detect (H) *ptc* transcripts or to immunostaining to detect (G and I) CiFL and Col proteins. CiFL protein was stabilized, whereas *ptc* transcription and Col protein production were not affected. (**J** to **O**) Overexpression of

wdb at 25°C or *ckIa* RNAi at 18°C, driven by *MS1096*-Gal4 (marked by box brackets), abolished the production of (L and O) Col protein, but (K and N) expanded the area of *dpp* expression. The wing discs were subjected to in situ hybridization to examine *dpp* transcription followed by immunofluorescence staining to visualize Col protein. (J and M) Merged images are shown, with *dpp* in red and Col in green. (**P** to **R**) Wing discs were subjected to in situ hybridization to detect (Q) *ptc* transcripts or to immunostaining to detect (P and R) CiFL and Smo proteins. When *ckIa* was inhibited by RNAi in the dorsal compartment (marked by box brackets), CiFL protein was stabilized, whereas *ptc* transcription was reduced. Smo protein was destabilized in the posterior compartment as a result of *ckIa* RNAi. Note that the area containing Smo protein was mildly expanded in the dorsal compartment along the AP boundary, which might be as a consequence of diminished *Ptc* expression in the corresponding region; see (Q).

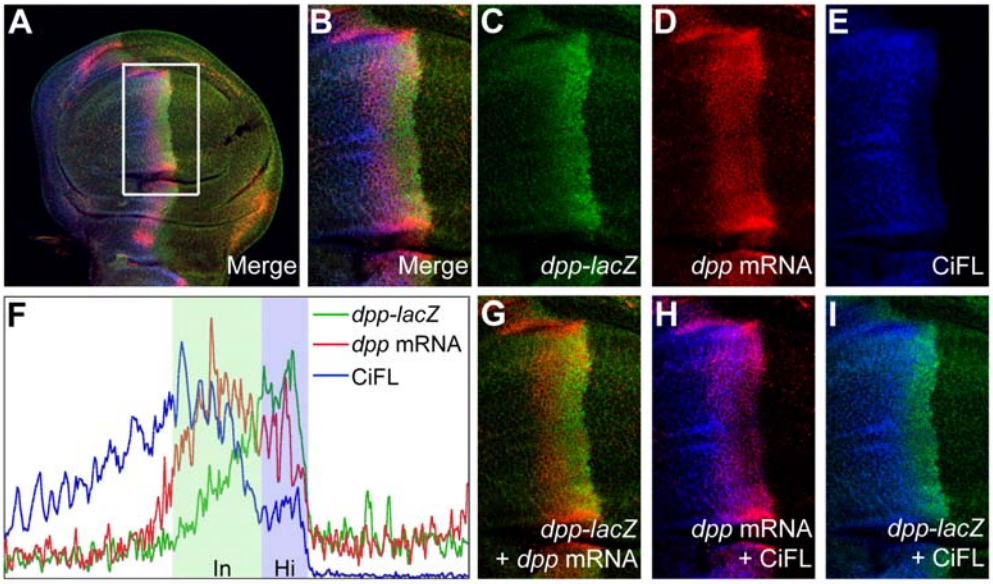

Fig. S5. Expression domains of *dpp* mRNA and a *dpp-lacZ* enhancer trap in a wild-type wing disc. (**A** to **E** and **G** to **I**) In a wild-type wing imaginal disc, (D) *dpp* mRNA (red) was detected by in situ hybridization followed by co-immunostaining with antibodies against (C) β-galactosidase (green) and (E) CiFL (blue) to visualize a *dpp-lacZ* enhancer trap and CiFL expression domains, respectively. (A and B) Three-color or (G to I) two-color merged views are also shown. The expression domains of (F) CiFL, *dpp-lacZ*, and *dpp* mRNA were analyzed with Image J software. The horizontal axis represents the AP orientation (anterior to the left, posterior to the right). Areas shaded in light blue and light green mark the high Hh-responsive (Hi) and low-to-intermediate Hh-responsive regions (In), respectively, based on the pattern of CiFL abundance (blue). Enhanced *dpp-lacZ* expression (green) was detected in the region of high Hh responsiveness, whereas enhanced *dpp* transcription (red) was detected in the region of intermediate Hh responsiveness. It is possible that activation of *dpp-lacZ* may require more intense Hh signaling activity than does the activaton of *dpp* transcription.

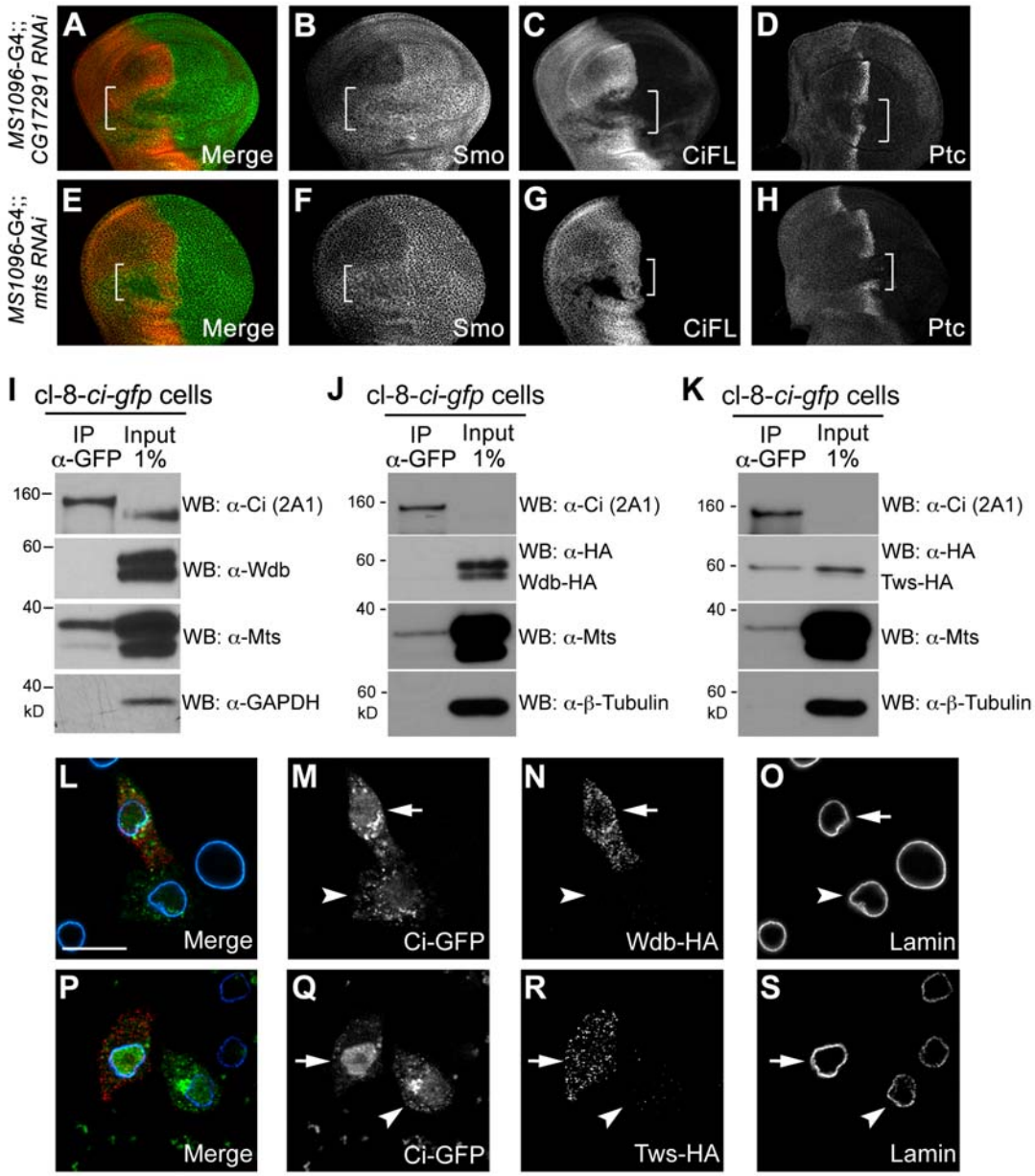

Fig. S6. Functional interaction between Ci and Tws-PP2A. (**A** to **H**) Dual roles for PP2A in regulating the stability of Smo and Ci. Inhibiting (A to D) the PP2A scaffolding A subunit (CG17291) or (E to H) the catalytic subunit (Mts) by RNAi under a *MS1096*-Gal4 driver (marked by box brackets) stabilized (B and F) Smo in the anterior compartment, but (C and G) destabilized CiFL protein. (D and H) The expression of the high-threshold Hh signaling target Ptc was abolished. (A) and (E) show the merged pictures for (B and C) and (F and G), respectively, with Smo in green and Ci in red. (**I** to **K**) Ci is associated with the PP2A regulatory subunit Tws, but not with Wdb. Protein lysates from cl-8 cells transiently transfected with *ci-gfp* alone or with *wdb-HA* or *tws-HA* were subjected to immunoprecipitation (IP) with agarose conjugated to antibody against GFP, and then analyzed by Western blotting (WB) with the indicated antibodies (n = 3 experiments). Mts

associated with Ci-GFP; however, only (K) Tws-HA, but not (I) endogenous Wdb or (J) Wdb-HA, was detected in an immunocomplex with Ci-GFP, suggesting that PP2A may function on Ci through Tws, but not Wdb. Cell lysate input (1%) was loaded as indicated. Note that the 2A1 antibody was only able to detect ectopically expressed Ci-GFP after immunoprecipitation (the slower migrating form). The faster migrating endogenous Ci is shown in the 1% input in (I). (**L** to **S**) Tws translocates Ci to the nucleus. cl-8 cells were transiently transfected with *ci-gfp* together with (L to O) *wdb-HA* or (P to S) *tws-HA*. (M and Q) Ci-GFP was directly visualized in cl-8 cells (green). (N) Wdb-HA (red) and (R) Tws-HA (red) were detected with an antibody against HA. (O and S) An antibody against lamin was used to mark the nuclear envelop (blue). (L) and (P) are merged images of panels (M to O) and (Q to S), respectively. (M) Wdb-HA did not affect the localization of Ci-GFP localization (arrow); however, (Q) Tws-HA localized Ci-GFP to the nucleus (arrow). Cells co-expressing *ci-gfp* and *wdb-HA* or *tws-HA* are marked with arrows. Cells expressing *ci-gfp* alone are indicated by arrowheads.

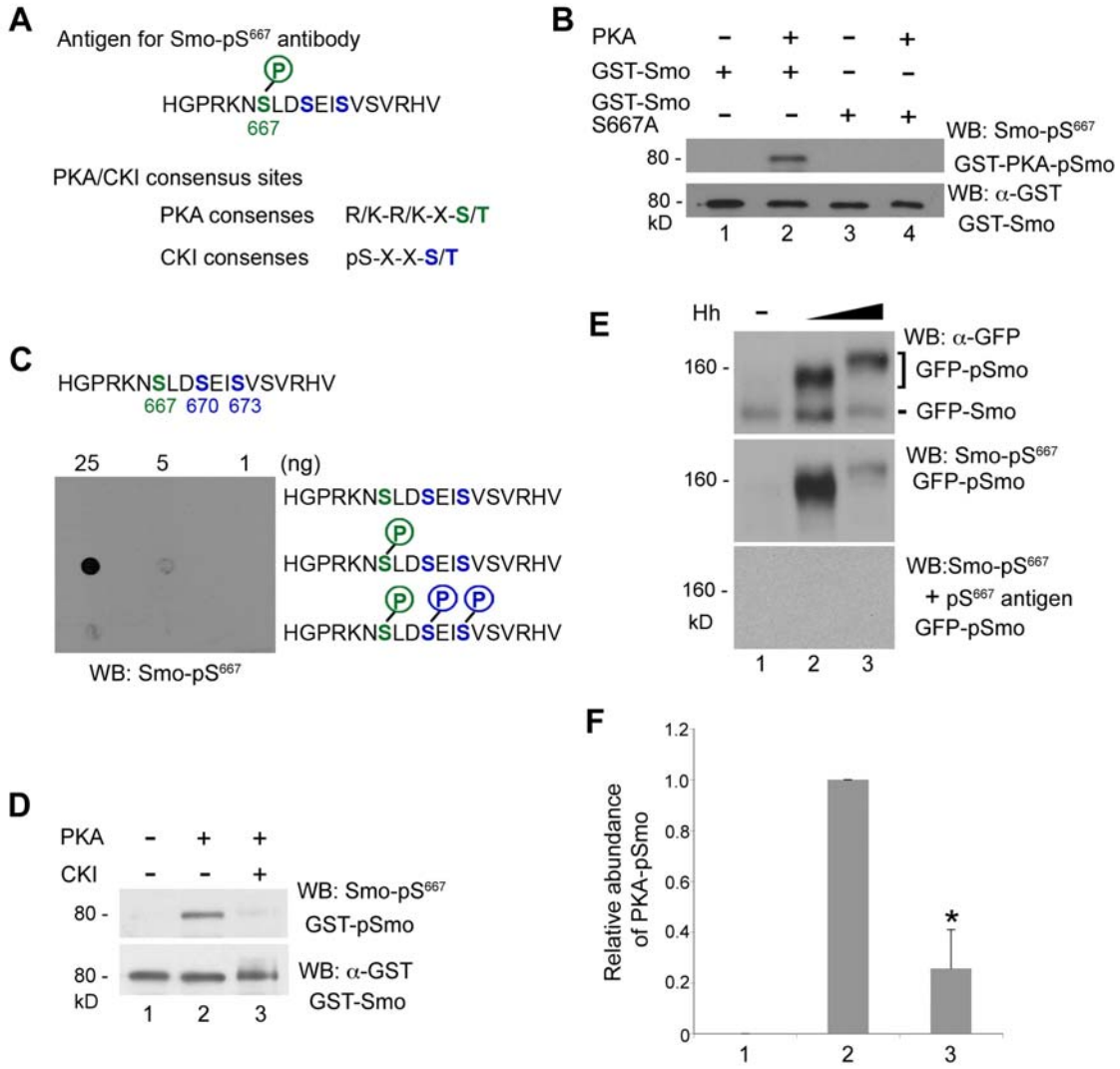

Fig. S7. Characterization of the phosphospecific antibody α-Smo-pS^{667} . (**A**) The phosphorylated peptide used to generate a rabbit polyclonal antibody against phosphorylated Smo (Smo-pS^{667}) corresponding to amino acid residues 661 to 679 within the first PKA-CKI cluster of fly Smo. Ser^{667} was phosphorylated to mimic PKA phosphorylation. Also shown are the PKA and CKI phosphorylation consensus sites, which are highlighted in green and in blue, respectively. (**B**) The recognition of Smo by the α-Smo-pS^{667} antibody is limited to PKA modification within cluster 1. The Smo-pS^{667} antibody specifically recognized PKA-phosphorylated wild-type Smo (lane 2) but not a GST-Smo^{S667A} mutant in which Ser^{667} was mutated to alanine. Detection of GST was used to control for equal loading. (**C**) The peptide or (**D**) a GST-Smo 557-1036 fusion protein were treated with PKA, CKI, or both, as indicated. The Smo-pS^{667} antibody specifically recognized the PKA-phosphorylated peptide and GST-Smo, but poorly detected the PKA primed, CKI-phosphorylated peptide or GST-Smo. Unphosphorylated peptide or GST-Smo were not detected by Smo-pS^{667}. (C) The amount of peptides spotted onto the nitrocellulose is indicated. (D) Detection of GST served as the loading control. (**E** and **F**)

cl-8-*gsmo* cells were treated with increasing amounts of Hh-conditioned medium. Western blotting (WB) analysis with an antibody against GFP (top panel) was performed to detect unphosphorylated GFP-Smo and all forms of phosphorylated GFP-Smo (GFP-pSmo). The Smo-pS^{667} antibody (middle panel) detected phosphorylated GFP-Smo (presumably GFP-PKA-pSmo). This detection was eliminated by competition of the Smo-pS^{667} antibody with the Smo-pS^{667} antigen (lower panel). (E) A single representative experiment is shown. The enhanced phosphorylated Smo (lane 3), which was induced by an enhanced amount of Hh, exhibited slower migration than did intermediate-phosphorylated Smo (lane 2). (F) The relative abundances of GFP-PKA-pSmo (detected by the Smo-pS^{667} antibody) among all forms of GFP-pSmo (detected by the GFP-specific antibody) in response to Hh activation in 7 independent experiments were measured with Image J software (F). Enhanced phosphorylated Smo contains about 5-fold less PKA-phosphorylated Smo than does intermediate pSmo. *, $P < 0.005$.

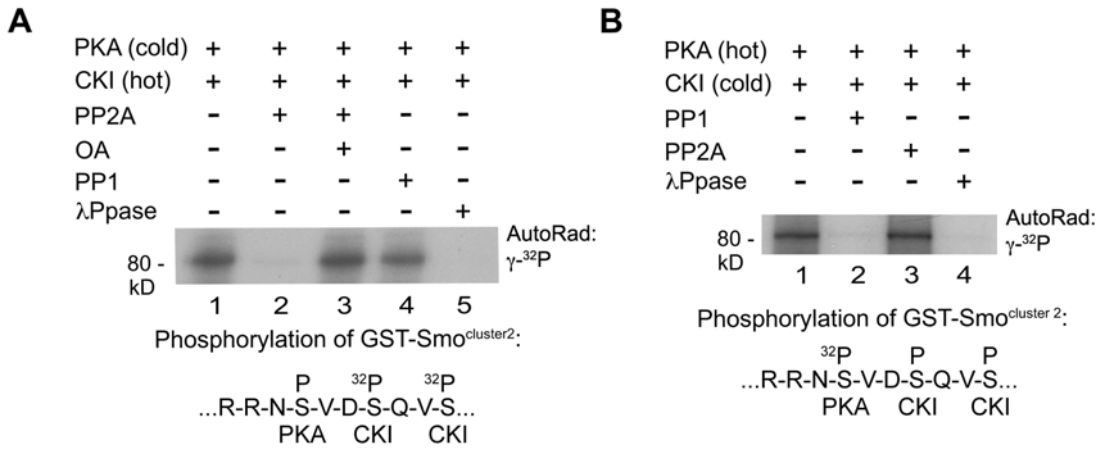

Fig. S8. PP2A specifically dephosphorylates CKI-phosphorylated Smo. (**A**) GST-Smo^{cluster2} was phosphorylated with PKA in the presence of cold ATP followed by phosphorylation by CKI in the presence of [γ-^{32}P]-ATP (lane 1), which resulted in the selective incorporation of the radiolabel only into the CKI consensus serines in PKA-CKI cluster 2, as shown. CKI phosphorylation–specific ^{32}P-phosphates were removed by PP2A (lane 2), but not by PP1 (lane 4). OA was used to inhibit PP2A activity (lane 3), whereas λPpase was used as a positive control (lane 5). (**B**) GST-Smo^{cluster2} was phosphorylated with PKA in the presence of [γ-^{32}P]-ATP followed by phosphorylation with CKI in the presence of cold ATP (lane 1), which resulted in the selective incorporation of radiolabel only into PKA consensus serines in cluster 2, as shown. PKA phosphorylation–specific ^{32}P-phosphates were removed by PP1 (lane 2), but not by PP2A (lane 3). λPpase was used as positive control in (lane 5).

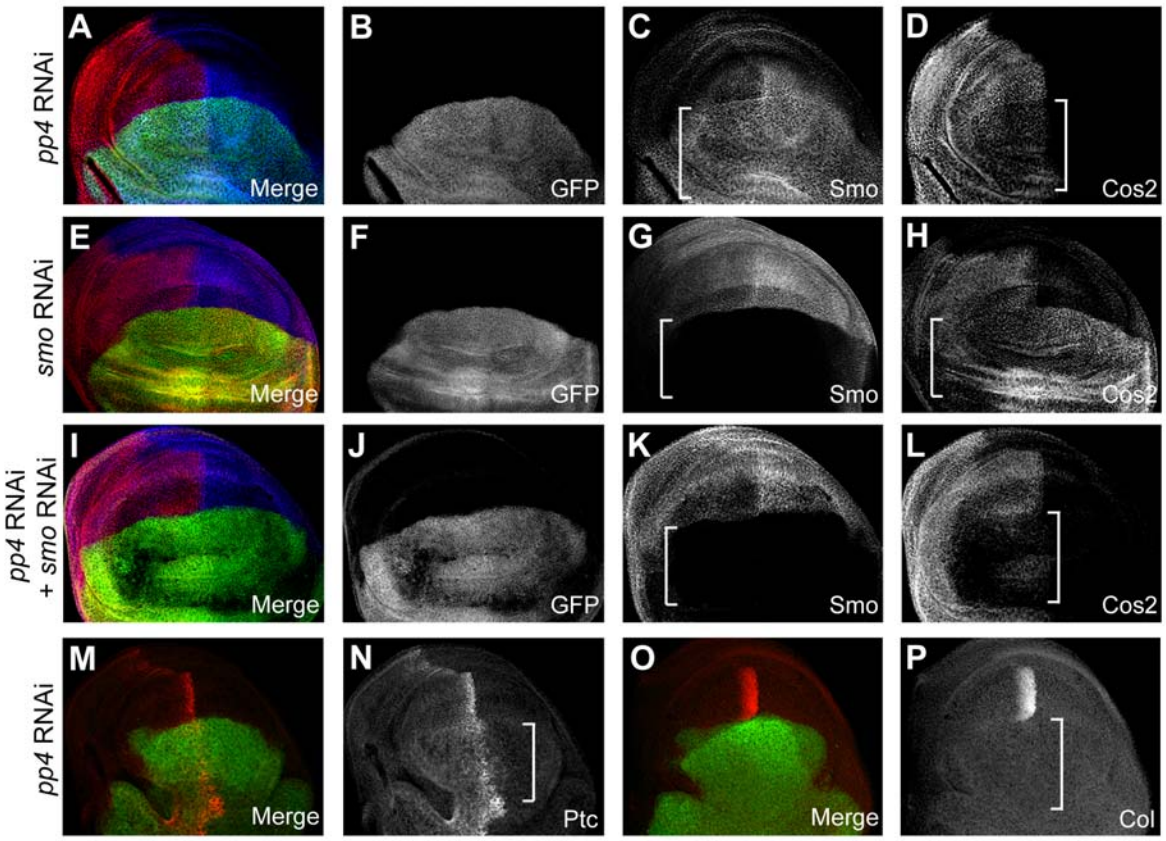

Fig. S9. The role of PP4 in regulating Hh signaling. *smo* RNAi, *pp4* RNAi, or both were expressed at 18°C in the dorsal compartment of the wing disc driven by *ap*-Gal4 (indicated by box brackets), and marked by GFP. (**A** to **L**) Genetic relationship between *pp4* and *smo*. Inhibition of PP4 activity by RNAi stabilizes (C) Smo, but reduced the abundance of (D) Cos2. (G) In contrast, knockdown of *smo* expression by RNAi promoted (H) the production of Cos2. (L) Inhibition of *pp4* and *smo* by RNAi abolished Cos2 production, suggesting that PP4 acts downstream of Smo. (**M** to **P**) Manipulating PP4 activity altered the expression of Hh-responsive genes. (P) Reducing *pp4* expression by RNAi abolished the production of Col. (N) The abundance of Ptc protein was also reduced at the AP boundary.

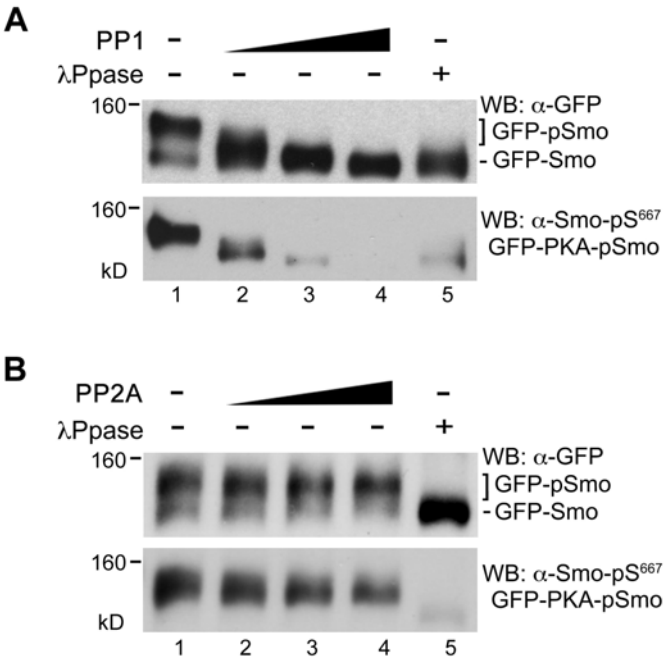

Fig. S10. Distinct abilities of PP1 and PP2A to dephosphorylate moderately-phosphorylated Smo. Lysates of cl-8-*gsmo* cells treated with intermediate-threshold Hh (equivalent to exposure to 50% Hh-CM) were treated with increasing amounts of (A) PP1 or (B) PP2A. Western blotting analysis with an antibody against GFP (top panels) detected all forms of GFP-pSmo (box brackets), which were completely removed by λ-phosphatase (λPpase). The α-Smo-pS^{667} antibody (bottom panels) specifically recognized GFP-PKA-pSmo. (A) PP1 efficiently dephosphorylated moderate-phosphorylated GFP-Smo, whereas (B) PP2A had little ability to dephosphorylate GFP-PKA-pSmo (n = 3 experiments).

Table S1. T7-primed primers used to construct the PSTP dsRNA library.

Type of Phospha -tase	CG Number	Name	Forward (5`) and Reverse (3`) Primers
PPP	1455	CanA1	5' taatacgactcactatagggTCGAGGAAGAGCTACGCAAGAAAAT 3' taatacgactcactatagggTCATTACTGCTGGTGTTGCTGATGT
	1459	PP4-19C	5' taatacgactcactatagggGCTGTTCAAGGTTGGCGGCGATGTG 3' taatacgactcactatagggGATATCGTTCGTGCGGTTGAACTGG
	2096	PP1-Flw	5' taatacgactcactatagggGCAAGCGCCGATACAATGTCAAACT 3' taatacgactcactatagggCGCTGTACAGATACTTGGCCTTCTT
	3245	PPN-58A	5' taatacgactcactatagggATACACGGTCAGTACCTAAATC 3' taatacgactcactatagggGAAGGCACTGACCACATCT
	5650	PP1-87B	5' taatacgactcactatagggCGATCTGTTGCGTCTGTTC 3' taatacgactcactatagggCTCGTGCTTCTGCAAAAAC
	6571	RdgC (PP7)	5' taatacgactcactatagggCACGGATAGTCAAAAGGTTAACTAT 3' taatacgactcactatagggACTTCTTAGGATCGATTACTTTGGA
	6593	PP1-96A	5' taatacgactcactatagggAGATCCGCAGCCTGTGCCTCAAGTC 3' taatacgactcactatagggACCACAGCAGATCGCACAGCAGTCC
	7109	Mts/ PP2A-C	5' taatacgactcactatagggAAATGCCCGGTGACAGTG 3' taatacgactcactatagggCACGAGGCGAGATTCCC
	8402	PPD3 (PP5)	5' taatacgactcactatagggTGGAGTGTATATTTACGCTGTTTGG 3' taatacgactcactatagggTATCACAATAGTTCGGAGCAGAGAA
	8822	PPD6	5' taatacgactcactatagggAGTTGTGGGCGACATACAC 3' taatacgactcactatagggGGACATCGCGACCATAGA
	9156	PP1-13C	5' taatacgactcactatagggATGATCTGTTGCGTCTGTTC 3' taatacgactcactatagggTGCTTTTGGAGGAACTTGAC
	9819	CanA-14F	5' taatacgactcactatagggCAAGTATCTGTTCCTGGGCGACTAC 3' taatacgactcactatagggCGGATGATCGACAGCAGGTTGTTGT
	9842	PP2B-14D	5' taatacgactcactatagggGCGGAAGCCACAGATGCCAATAGTA 3' taatacgactcactatagggACAGGACGCACTCGATGCTGAAGTA
	10138	PPD5	5' taatacgactcactatagggTCCTGCTGCGCGGCAATCATGAATC 3' taatacgactcactatagggACCAGTTTGGCGTCCACCACCAGAA

	10930	PPY-55A	5' taatacgactcactatagggTCACGAGAGCGCCAGTATAAATAAA 3' taatacgactcactatagggATAATGACGAAGGAGCAGATCAAGT
	11597		5' taatacgactcactatagggAGGAGCATCGCTACTTGTT 3' taatacgactcactatagggATCCTGGGCCAACTGATGA
	12217	PPV	5' taatacgactcactatagggCCGCATACCAACTACATATTC 3' taatacgactcactatagggCTCGGCATATGAGGTTCAG
PPM	1906	Alph	5' taatacgactcactatagggCTTCCTGCGCATCGACGAGGTTATG 3' taatacgactcactatagggACGACCTGGTTGGCGATGCTCACTA
	2984	PP2C1	5' taatacgactcactatagggCTTCCGCAACTTCGACTAC 3' taatacgactcactatagggGGAATGGGCAGTGGTTTGT
	6036		5' taatacgactcactatagggAGTTGGATGAGGATATGAGGA 3' taatacgactcactatagggTTGTCCCTGCTGCCTTTAT
	7115		5' taatacgactcactatagggGTCATGGCGGCGAGTTT 3' taatacgactcactatagggTCTTGGCCTGCTCCACAA
	10376		5' taatacgactcactatagggCACATCTGCCGCTGTAAAGAACAAA 3' taatacgactcactatagggTAAGAATGCCATTTACACGCCACTG
	10417		5' taatacgactcactatagggAAGCTACTAATAAAGCTGTAATG 3' taatacgactcactatagggTCACCGTCGTCATCATTTTC
	10493	Phlpp	5' taatacgactcactatagggAGGTTTGTCAGAGCCAGAG 3' taatacgactcactatagggGGTAGGCGTCCAGACCTC
	12151	Pdp	5' taatacgactcactatagggGTTGCCTGTTTGGTTCACATT 3' taatacgactcactatagggATCGGTTCGAGGATCTTTTT
	12169	Ppm1	5' taatacgactcactatagggTGAGGTGGCCTTGAAAAAG 3' taatacgactcactatagggAGTTCCTCGCAAATGAGTTC
	17598		5' taatacgactcactatagggCATGCGTGGCTGGACATACAAAACT 3' taatacgactcactatagggCTCCACGTGCTCTTTGTAATACTGG
	17746		5' taatacgactcactatagggCGTTATGCTACGCAACAAG 3' taatacgactcactatagggCCGAGGCCTCCCATTTG
DSP	1395	Stg	5' taatacgactcactatagggGGCCAGATCAAGGAGCAG 3' taatacgactcactatagggAGCGGCAGTCGATGATG
	1810	mRNA-capping-	
			5' taatacgactcactatagggGGCAACGGCGATGGTTT 3' taatacgactcactatagggAGAGTGCCGTCGAGATG

		enzyme	
	3530		5' taatacgactcactatagggCCAACGCCGTGGACAAG 3' taatacgactcactatagggGTGCCAGGTTGGCCTTAA
	3632		5' taatacgactcactatagggAGCCGCCATGAGCAATC 3' taatacgactcactatagggGATTTCATCCAGCGTGAGTT
	4965	Twe	5' taatacgactcactatagggGAATCAGCCGAGAATCACAA 3' taatacgactcactatagggGAAACGCCTCCTGTATCTG
	4993	PRL-1	5' taatacgactcactatagggCAAGGCATTACCGTCAAGGACC 3' taatacgactcactatagggTTTTGGGCTCTCTGTGGTTAGTTC
	5671	Pten	5' taatacgactcactatagggATGTCCAACGTGATACGCAATGTAGT 3' taatacgactcactatagggTTGTCACACCTTTTCGGTCCTTTGTA
	6238	Ssh	5' taatacgactcactatagggGATGAGAAGACGAACCTGC 3' taatacgactcactatagggGGTTTTGGGTGATGTGCTG
	7134	Cdc14	5' taatacgactcactatagggCGGGATTCTTTAATTTCAACG 3' taatacgactcactatagggCCACTGCTGCTGATGTCC
	7378		5' taatacgactcactatagggTCGCAAAAAAGTGCCCGTC 3' taatacgactcactatagggTGTCCAGTGTCCACCTGACCATAC
	7850	Puc	5' taatacgactcactatagggGATGCACGGAAAACGGGT 3' taatacgactcactatagggGCTGCCGCCGAAGTG
	9115	Mtm	5' taatacgactcactatagggTTGACCATCATGGATGCGCGACCAAG 3' taatacgactcactatagggTTGCAGGAACACCGGAGATCTGTCTG
	10089		5' taatacgactcactatagggTCGCGAAGGCAACGTAC 3' taatacgactcactatagggGTCATTGTTCGGATCCTTTTTA
	10371	Plip	5' taatacgactcactatagggCTGCTGTACAATGTCCTGATGGAAA 3' taatacgactcactatagggATTGTTTGGTGTGCAGCAGAATGTG
	13197		5' taatacgactcactatagggTCGTGTTCCTGGCACTCGTTTC 3' taatacgactcactatagggATCTCCTCTCTGTGGCAGCAAG
	14080	Mkp3	5' taatacgactcactatagggGGACGATAATCAGACGCACAGCAAAGA 3' taatacgactcactatagggATCAAGTAGGCGAGCGTCACGGTCAC
	14211		

5' taatacgactcactatagggTCCACTGTGATCGCTTACA

			3' taatacgactcactatagggCGGATGCGCTCGGAC
	15528		5' taatacgactcactatagggGGATCACACGCCGTTTCC 3' taatacgactcactatagggCTCGGGCTCCAGTATGTC
PP2A A subunit	17291		5' taatacgactcactatagggGACTTCTGCGCCAATCTGGAC 3' taatacgactcactatagggATCAATGACGCTGGCCTCCAG
			5' taatacgactcactatagggGGCACAGGATGATCAGGACT 3' taatacgactcactatagggGTCGTTAACGCAATCCAGGT
PP2A C subunit	7109	Mts	5' taatacgactcactatagggAAGCGGCTCTTATGGAACTGG 3' taatacgactcactatagggCCTTCTGCTCCTCCCCTTTATC
			5' taatacgactcactatagggAAATGCCCGGTGACAGTG 3' taatacgactcactatagggCACGAGGCGAGATTCCC
PP2A B subunits	5643	Wdb	5' taatacgactcactatagggGAGGACGATCCGACACTGGAG 3' taatacgactcactatagggCATGATCGGCATGATGACCGC
			5' taatacgactcactatagggTCCAGCCTAGAACAGGAGGA 3' taatacgactcactatagggTTTCCAAGAGCTCACCGACT
	6235	Tws	5' taatacgactcactatagggGTTAATTCGGATCAGGAGACC 3' taatacgactcactatagggTATGAAGAGGTTATTGGTCGC
	7913	Wrd	5' taatacgactcactatagggTCCAACCCGAATGGTGCC 3' taatacgactcactatagggGCGACATAATGTACTCGTTGTTC
	4733		5' taatacgactcactatagggAGATTCCGTTCGTACATCGTG 3' taatacgactcactatagggGAAGGTATCGAAGAAGACGTG